2013

Recruitment dynamics in adaptive social networks

Maxim S. Shkarayev
William & Mary, mshkarayev@wm.edu

Leah B. Shaw
William & Mary, lbshaw@wm.edu

Ira B. Schwartz

PAPER

Recruitment dynamics in adaptive social networks

To cite this article: Maxim S Shkarayev *et al* 2013 *J. Phys. A: Math. Theor.* **46** 245003

View the article online for updates and enhancements.

IOP ebooks™

Bringing you innovative digital publishing with leading voices to create your essential collection of books in STEM research.

Start exploring the collection - download the first chapter of every title for free.

Recruitment dynamics in adaptive social networks

Maxim S Shkarayev[1]**, Ira B Schwartz**[2] **and Leah B Shaw**[1]

[1] Applied Science Department, College of William and Mary, Williamsburg, VA 23187, USA
[2] Nonlinear Systems Dynamics Section, Plasma Physics Division, Code 6792,
US Naval Research Laboratory, Washington, DC 20375, USA

E-mail: shkar@iastate.edu

Abstract

We model recruitment in adaptive social networks in the presence of birth and death processes. Recruitment is characterized by nodes changing their status to that of the recruiting class as a result of contact with recruiting nodes. Only a susceptible subset of nodes can be recruited. The recruiting individuals may adapt their connections in order to improve recruitment capabilities, thus changing the network structure adaptively. We derive a mean-field theory to predict the dependence of the growth threshold of the recruiting class on the adaptation parameter. Furthermore, we investigate the effect of adaptation on the recruitment level, as well as on network topology. The theoretical predictions are compared with direct simulations of the full system. We identify two parameter regimes with qualitatively different bifurcation diagrams depending on whether nodes become susceptible frequently (multiple times in their lifetime) or rarely (much less than once per lifetime).

PACS numbers: 87.10.Mn, 05.10.Gg

(Some figures may appear in colour only in the online journal)

1. Introduction

Any society contains individuals who are carriers of an ideology or fad (e.g., a religious or political party affiliation) that they desire to spread to the rest of the society. Thus, for a given ideology, a society can be partitioned into a set of people that represent the ideology and want to spread it, and the complement of this set. For example, the ideology could correspond to the views of a particular political party, with the party members desiring to recruit new members to improve their positions in the government. Other areas of recruitment have been proposed as mechanisms for fads which appear as a rapid rise above some threshold, as in music [1], management technologies [2], economics [3], and even science [4]. Slower recruitment based on social networks has been postulated in biology [5] and the spread of alcoholism [6]. Slowing

the rise of a fad or eliminating the spread of an ideology has been also been proposed through the control of critical nodes in a social network [7].

In today's world where collisions between ideologies can lead to radicalization of society, the problem of existence and formation of terrorist networks or insurgency movements becomes important. Recently, mathematical modeling of various radical groups, such as terrorist organizations, has been done to explore their structure and dynamics [8–11]. In addition to dynamical approaches that measure rates of attacks of radical groups [12], operations research theories have also been applied to the formation of radical groups [13]. Another class of works [14–16] focuses on the recruitment dynamics of terrorists within a well-mixed population using compartmental models similar to those used for epidemic spread. In [16][3], a systematic analysis of recruitment to Hezbollah has been done. Data from a political science discipline is used to generate a compartmental model of recruitment. Although the modeling is deterministic, it considers the various parameters which explicitly affect the success of recruitment to the radical's cause. Finally, a number of recent publications discuss terrorist networks as optimal structures that optimize communication efficiency while balancing the secrecy of the networks [17–19].

Not considered previously is the combination of the spread of radical ideas plus adaptive changes in social connections to improve recruitment success to the radical cause. Some work in this direction is presented in the papers studying voter models in which individuals make connections to influence others' opinions [20–22], as well as opinion dynamics models in which individuals are influenced by neighbors' opinions [23].

We develop a simple model of a society in which some of the members belong to a class that tries to spread an ideology. The ideology spreads as a result of contact of recruiting members with nonrecruiting members. The recruiting members may improve their chances to recruit via network adaptation. The purpose of the adaptation proposed here is to improve the spread of the ideology, which is in contrast to network adaptation in epidemiological models [24, 25] where the purpose is avoidance of contact with the spreading members. In addition to adaptation, the connectivity within the society changes due to birth of new members and death of existing members. Using this model, we explore how the existence of stable recruiting classes depends on the adaptation and other parameters. We also consider the network topology of the recruiting class, as it may be important in assessing the quality of the communication channels in the resulting structure. Section 2 presents the model and a system of mean-field equations describing its dynamics. Section 3 presents mean-field analysis of the threshold for successful recruiting and its dependence on the network adaptation. These results are compared with simulations of the full system, and the network geometry of the recruiting class is considered. Section 4 concludes.

2. Modeling the dynamics of recruitment

2.1. Model

We consider a social structure consisting of M individuals represented by nodes in a network. An existing relation between any two individuals is represented by a link between the two nodes. New individuals join the society at a constant total rate μ, and the individuals in the network can leave the network via death at rate δ per individual. When new individuals join the system, they arrive with σ links, which are connected to σ randomly selected nodes in the population. When individuals die, their links are removed.

---

[3] Contains many good references for recruitment, both stochastic and deterministic.
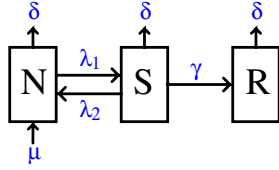
Figure 1. Schematic representation of node fluxes in and out of the network due to birth and death, described by the rates μ and δ respectively. Fluxes between the three classes are described by the transition rates λ_1, λ_2 and γ. Link rewiring (not shown here) takes place at rate w. New nodes are generated with σ links to existing nodes.

Some members of the society, *recruiters* (also referred to as R-nodes), are carriers of an ideology that they try to spread to the individuals they come into contact with. The individuals that do not belong to the recruiting class are divided into two groups: those who are *susceptible* to the recruitment (S-nodes) and those who are *non-susceptible* (N-nodes). We assume that individuals can spontaneously change their state from non-susceptible to susceptible and vice versa (with rates λ_1 and λ_2 respectively). An individual in the recruiting class remains in that class until death [14].

A susceptible individual joins the recruiting class at a rate that is proportional (with proportionality constant γ) to the number of contacts it has with the recruiting class. In order to improve their recruiting capabilities, the recruiting individuals can rewire their links with rate w, abandoning any connection to a non-susceptible individual in favor of a connection to a susceptible one that is randomly selected from the susceptible population. As the links are rewired, the network topology changes based on the current states of its nodes. A schematic representation of the node dynamics is shown on figure 1.

We perform Monte Carlo simulations of the above system following the continuous time algorithm described in [26]. We start with an Erdos–Renyi random network, which then evolves according to the rules of birth, death and rewiring. The results presented in the rest of the paper are for the systems that have reached a steady state.

2.2. Mean field

To describe the dynamics of this system, we construct a mean-field model for nodes and links (also referred to as a pair approximation) as in [24]. The time evolution of the nodes of each type is described by the following rate equations:

$$\partial_t \mathcal{N}_N = \mu - \lambda_1 \mathcal{N}_N + \lambda_2 \mathcal{N}_S - \delta \mathcal{N}_N \tag{1a}$$

$$\partial_t \mathcal{N}_S = \lambda_1 \mathcal{N}_N - \lambda_2 \mathcal{N}_S - \gamma \mathcal{N}_{RS} - \delta \mathcal{N}_S \tag{1b}$$

$$\partial_t \mathcal{N}_R = \gamma \mathcal{N}_{RS} - \delta \mathcal{N}_R, \tag{1c}$$

Here the functions $\mathcal{N}_N \equiv \mathcal{N}_N(t)$, $\mathcal{N}_S \equiv \mathcal{N}_S(t)$, $\mathcal{N}_R \equiv \mathcal{N}_R(t)$ represent the number of nodes of each type. The process of recruitment is captured by the $\gamma \mathcal{N}_{RS}$ term, where the recruitment is shown to take place at a rate proportional to the number of links between the recruiting class and the susceptible class, $\mathcal{N}_{RS}$.

In order to capture the rewiring process, we follow the evolution of the number of different types of links present in the network:

$$\partial_t \mathcal{N}_{NN} = \lambda_2 \mathcal{N}_{SN} + \sigma\mu \frac{\mathcal{N}_N}{\mathcal{N}_N + \mathcal{N}_S + \mathcal{N}_R} - 2(\lambda_1 + \delta)\mathcal{N}_{NN} \tag{2a}$$

$$\partial_t \mathcal{N}_{\text{SN}} = \sigma\mu \frac{\mathcal{N}_{\text{S}}}{\mathcal{N}_{\text{N}} + \mathcal{N}_{\text{S}} + \mathcal{N}_{\text{R}}} - \gamma\mathcal{N}_{\text{NSR}} + 2\lambda_2\mathcal{N}_{\text{SS}} - (\lambda_1 + \lambda_2 + 2\delta)\mathcal{N}_{\text{SN}} + 2\lambda_1\mathcal{N}_{\text{NN}} \qquad (2b)$$

$$\partial_t \mathcal{N}_{\text{SS}} = -\gamma\mathcal{N}_{\text{SSR}} + \lambda_1\mathcal{N}_{\text{SN}} - 2(\lambda_2 + \delta)\mathcal{N}_{\text{SS}} \qquad (2c)$$

$$\partial_t \mathcal{N}_{\text{RN}} = \gamma\mathcal{N}_{\text{NSR}} + \sigma\mu \frac{\mathcal{N}_{\text{R}}}{\mathcal{N}_{\text{N}} + \mathcal{N}_{\text{S}} + \mathcal{N}_{\text{R}}} - (\lambda_1 + 2\delta + w)\mathcal{N}_{\text{RN}} + \lambda_2\mathcal{N}_{\text{RS}} \qquad (2d)$$

$$\partial_t \mathcal{N}_{\text{RS}} = -\gamma\mathcal{N}_{\text{RSR}} + \gamma\mathcal{N}_{\text{SSR}} - (\lambda_2 + 2\delta)\mathcal{N}_{\text{RS}} + (\lambda_1 + w)\mathcal{N}_{\text{RN}} \qquad (2e)$$

$$\partial_t \mathcal{N}_{\text{RR}} = \gamma\mathcal{N}_{\text{RSR}} - 2\delta\mathcal{N}_{\text{RR}}, \qquad (2f)$$

where the terms $\mathcal{N}_{xy}$ correspond to the number of links connecting nodes from classes x and y, e.g., $\mathcal{N}_{\text{NN}}$ corresponds to the number of NN links. The terms proportional to $\sigma\mu$ correspond to the influx of edges due to the birth of new nodes, where the probability for the new node to attach itself to a node from class X is proportional to the number of nodes in that class. The third order terms, $\mathcal{N}_{\text{NSR}}$, $\mathcal{N}_{\text{SSR}}$ and $\mathcal{N}_{\text{RSR}}$, describe the formation of triples of nodes with an S-node at the center, and at least one of the edges terminating at an R-node. These terms describe the rate at which NS-, SS- and RS-links become NR-, SR- and RR- links respectively, due to the interaction of the central S-node with its neighboring R-node. Note that our definition of RSR triples includes *degenerate* triples, i.e., RSR triples where both of the R-nodes correspond to a single R-node, by analogy with degenerate triangles.

The resulting system of equations is not closed, as it contains higher order terms. Following earlier works in epidemiology [27], we introduce the closure based on the assumption of homogeneous distribution of R-nodes in the neighborhood of S-nodes:

$$\mathcal{N}_{\text{NSR}} = \frac{\mathcal{N}_{\text{RS}}}{\mathcal{N}_{\text{S}}} \frac{\mathcal{N}_{\text{SN}}}{\mathcal{N}_{\text{S}}} \mathcal{N}_{\text{S}}, \qquad (3a)$$

$$\mathcal{N}_{\text{SSR}} = \frac{\mathcal{N}_{\text{RS}}}{\mathcal{N}_{\text{S}}} \frac{2\mathcal{N}_{\text{SS}}}{\mathcal{N}_{\text{S}}} \mathcal{N}_{\text{S}}. \qquad (3b)$$

For example, the number of NSR triples is assumed to be the product of the number of S-nodes, the average number of N neighbors of an S-node, and the average number of R neighbors of an S-node. With an additional assumption that the total degree distribution of S-nodes, $P_S(d)$, is given by the Poisson distribution, we conclude that the number of R-nodes in the neighborhood of S-nodes is also Poisson. That is, the homogeneity assumption corresponds to the binomial distribution of the number of R-nodes in the neighborhood of an S-node with total degree d, and, therefore, the probability that k R-nodes are in the neighborhood of an S-node is given by

$$\sum_d P_S(d)B(d,p) = \sum_d \frac{e^{-\psi}\psi^d}{d!} \binom{n}{k}\phi^k(1-\phi)^{n-k} = \frac{e^{-\phi\psi}(\phi\psi)^k}{k!}, \qquad (3c)$$

where $\psi = (\mathcal{N}_{\text{SN}} + 2\mathcal{N}_{\text{SS}} + \mathcal{N}_{\text{RS}})/\mathcal{N}_{\text{S}}$ is the mean degree of S-nodes and $\phi = \mathcal{N}_{\text{RS}}/(\mathcal{N}_{\text{SN}} + 2\mathcal{N}_{\text{SS}} + \mathcal{N}_{\text{RS}})$ is the probability that a randomly chosen neighbor of S-node is an R-node. Thus, the closure of $\mathcal{N}_{\text{RSR}}/\mathcal{N}_{\text{S}}$ follows from the relation between first moment, $\mathcal{N}_{\text{RS}}/\mathcal{N}_{\text{S}}$, and second moment, $\mathcal{N}_{\text{RSR}}/\mathcal{N}_{\text{S}}$, of the Poisson distribution:

$$\mathcal{N}_{\text{RSR}} = \left(\left(\frac{\mathcal{N}_{\text{RS}}}{\mathcal{N}_{\text{S}}}\right)^2 + \frac{\mathcal{N}_{\text{RS}}}{\mathcal{N}_{\text{S}}}\right)\mathcal{N}_{\text{S}}. \qquad (3d)$$

We thus obtain a system of nine mean-field equations, which we analyze.

4

3. Results

3.1. Mean-field recruiting threshold

We first consider the bifurcation point of the recruitment model where the zero recruit (trivial) steady state becomes unstable, which we call the *recruiting threshold*. This is a transcritical bifurcation point, which is analogous to the epidemic onset in epidemic spreading models. It can be found analytically as a function of parameters for the mean-field model, and certain asymptotic limits have a simple form.

We nondimensionalize equations (1) and (2) to simplify the analysis. We introduce the dimensionless time variable $\tilde{t} \equiv \delta t$, where time is rescaled by the average node lifetime δ^{-1}. Further, the node variables are rescaled by the expected population size at steady state, μ/δ, while the link variables are rescaled by the expected number of links at steady state, $(\mu/\delta)(\sigma/2)$. Let $\mathbf{x} \equiv [\mathcal{N}_N, \mathcal{N}_S, \mathcal{N}_R, \mathcal{N}_{NN}2\sigma^{-1}, \mathcal{N}_{SN}2\sigma^{-1}, \mathcal{N}_{SS}2\sigma^{-1},$ $\mathcal{N}_{RN}2\sigma^{-1}, \mathcal{N}_{RS}2\sigma^{-1}, \mathcal{N}_{RR}2\sigma^{-1}]\delta\mu^{-1}$ denote the nine-dimensional vector of rescaled node and link state variables. Note that in the steady state the rescaled node variables sum to 1, and, therefore, in steady state they correspond to the probability for a node of a given type to exist in the system. Similarly, the rescaled link variables sum to 1, and correspond to the probability for an edge chosen at random to be of a given type, e.g., at steady state x_8 corresponds to the probability for a randomly chosen edge to be an RS link.

We introduce the following rescaled parameters:

$$\Lambda_1 \equiv \lambda_1\delta^{-1} \tag{4a}$$

$$\Lambda_2 \equiv \lambda_2\delta^{-1} \tag{4b}$$

$$\Gamma \equiv (\gamma\sigma/2)\delta^{-1} \tag{4c}$$

$$W \equiv w\delta^{-1}. \tag{4d}$$

We can now write the dimensionless equations of motion as

$$\dot{\mathbf{x}} = \mathbf{F}(\mathbf{x}; \bar{\Lambda}) \tag{5}$$

where $\bar{\Lambda} \equiv [\Lambda_1, \Lambda_2, W, \Gamma, \sigma]$ is a vector of all the system parameters. (Recall that σ is a dimensionless integer.) The full system of dimensionless equations is given in equations (A.1).

We can now find the trivial steady-state solution, where the number of R-nodes is zero. This restricts the state to be of the form $\mathbf{x}_0 = [x_{0,1}, x_{0,2}, 0, x_{0,4}, x_{0,5}, x_{0,6}, 0, 0, 0]$, where the number of links involving R-nodes is zero as well. This guarantees that $F_i(\mathbf{x}_0, \bar{\Lambda}) = 0$ for $i = 3, 7, 8, 9$. Since this subset of equations represents an invariant manifold, we concentrate on solving the equations for the rest of the five components, $x_{0,1}, x_{0,2}, x_{0,4}, x_{0,5}$ and $x_{0,6}$.

The first observation is that the x_1 and x_2 equations are solvable when the number of recruiting nodes is zero, and they yield steady-state values of

$$x_{0,1} = (\Lambda_2 + 1)D^{-1}, \tag{6a}$$

$$x_{0,2} = \Lambda_1 D^{-1}, \tag{6b}$$

where $D \equiv \Lambda_1 + \Lambda_2 + 1$. The nonzero link variables may be expressed in terms of $x_{0,1}, x_{0,2}$, and they are given by the following:

$$x_{0,4} = (\Lambda_2 + 1)^2 D^{-2}, \tag{6c}$$

$$x_{0,5} = 2\Lambda_1(\Lambda_2 + 1)D^{-2}, \tag{6d}$$

$$x_{0,6} = \Lambda_1^2 D^{-2}. \tag{6e}$$

Now that we have the full trivial solution, we can examine its stability. In order to do this, we linearize the vector field about $\mathbf{x_0}$ and examine where it has a one-dimensional null space. That is, at the bifurcation point, there is only one real eigenvalue passing through zero. This is equivalent to examining where the determinant of the Jacobian vanishes; i.e., we compute those parameters where

$$\det(\mathcal{D}_\mathbf{x}\mathbf{F}(\mathbf{x}_0, \bar{\Lambda})) = 0. \tag{7}$$

The following relation describes the location of the bifurcation:

$$W = -\Lambda_1 \left[1 + \frac{2\Gamma}{[\Gamma(2 - \sigma^{-1}) - 1](\Lambda_1 + \Lambda_2 + 1)} \right]$$
$$+ \Lambda_2 \frac{1}{\Gamma(2 - \sigma^{-1}) - 1} + \frac{2(\Gamma\sigma^{-1} + 1)}{\Gamma(2 - \sigma^{-1}) - 1} \tag{8}$$

We next examine the limits of equation (8) when either the recruitment rate Γ or rewiring rate W is large. The minimum amount of recruitment required to maintain nonzero values of recruited population, when W approaches infinity, can be found by setting the least common denominator of equation (8) to zero, which yields a simple expression for Γ:

$$\Gamma = \frac{1}{2 - \sigma^{-1}}. \tag{9}$$

If the recruitment rate is below this value, additional rewiring is not sufficient to enable spreading of the recruiting class.

Similarly, we find the smallest amount of rewiring required for existence of a nontrivial steady-state solution, conditioned on our ability to control Γ, with all the other parameters fixed:

$$\lim_{\Gamma \to \infty} W = -\Lambda_1 \left[1 + \frac{2}{(2 - \sigma^{-1})(\Lambda_1 + \Lambda_2 + 1)} \right] + 2\frac{\sigma^{-1}}{2 - \sigma^{-1}}.$$

For lower rewiring rates, the recruiting class cannot spread even if the recruiting rate is large. The value of this asymptote is greatest, meaning rewiring is most necessary, when Λ_1 approaches zero. In this case few non-susceptible nodes become susceptible to recruiting, and the necessary rewiring value approaches

$$W = \frac{2\sigma^{-1}}{2 - \sigma^{-1}}. \tag{10}$$

3.2. Comparison of mean field with simulations

We next compare the mean-field predictions for the spread of recruiters with simulations of the full stochastic network system. Thus, we compare the average size of the recruited portion of the population in statistical steady state to the solution of the mean-field equations at steady state, which we solve exactly in the appendix A. We assume that the parameters Λ_1 and Λ_2 (rates for gaining and losing susceptibility) depend on the openness of the society to a particular ideology and σ (determines average degree) depends on the typical number of contacts of an individual. On the other hand, we assume that the parameters Γ and W can be controlled by the recruiters, i.e., the recruiters may choose to be more or less aggressive in their recruitment, as well as in how quickly they rewire their links to susceptible members of society. Therefore, we investigate the recruiting effectiveness for a given choice of Λ_1, Λ_2 and σ, while varying Γ and W.
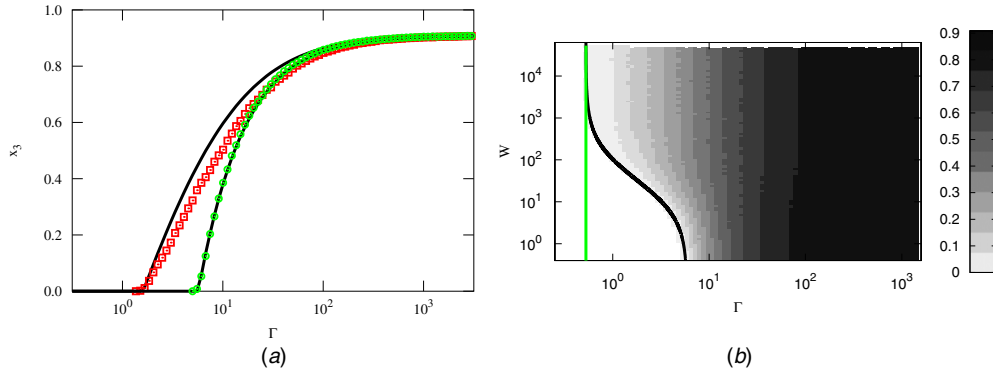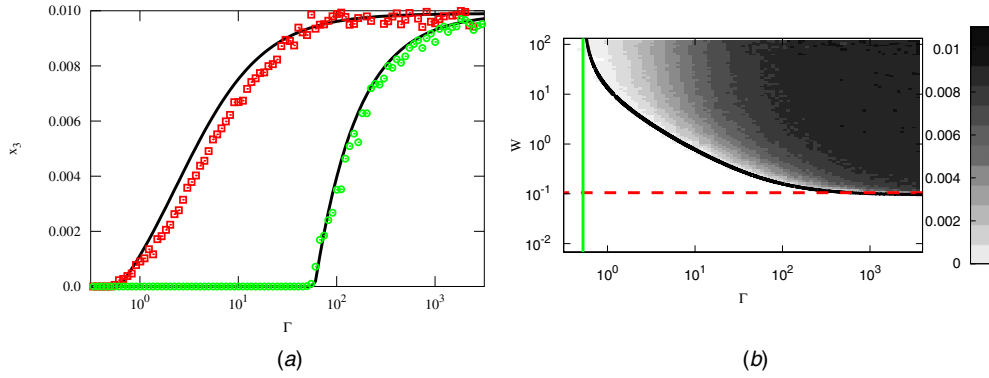
Figure 2. Direct numerical simulation of a stochastic network system with $\Lambda_1 \gg 1$. In (*a*) we compare the result of the simulation (symbols) to the mean-field solution given by equation (A.18) (solid curves). Square (red online): strong rewiring, $W \approx 40$. Circle (green online): weak rewiring, $W \approx 0.4$. (*b*) shows the density plot representing the dependence of the fraction of recruited nodes in the population in statistical steady state on rescaled rates of rewiring, W, and recruiting, Γ. Vertical solid line (green online) corresponds to the minimum recruitment rate required to support a nontrivial solution, as given by equation (9). The solid curve (black online) corresponds to the recruiting threshold as predicted by mean field in equation (8). The simulations are performed on a system with $\lambda_1 = 10, \lambda_2 = 100, \mu = 10^5, \delta = 1, \sigma = 10$. The time-averaged values are computed once the system reaches steady-state regimes. (In all of the figures in this paper this corresponds to at least $10\,\delta^{-1}$ units of time, in other words about ten generations of nodes have died before we observe the system to be at the steady state. The average is taken over 10^2 dynamical realizations.)

We distinguish two parameter regimes, corresponding to two qualitatively different behaviors of the system: small values of Λ_1 ($\Lambda_1 \ll 1$) and large values of Λ_1 ($\Lambda_1 \gg 1$). The small Λ_1 regime corresponds to the case where nodes become susceptible to recruiting only rarely, on average much less than once in their lifetime (where the average lifetime of a node is δ^{-1} in the original time units and 1 in the dimensionless $\tilde{t}$ units). The large Λ_1 regime corresponds to the case where, on average, nodes become susceptible to recruitment at least once in their lifetime.

We start with a random realization of Erdos–Renyi network of size 10^5 with 5×10^5 links. Each node is randomly assigned one of the three states, N, S or R, with the probability 0.85, 0.05, and 0.1 respectively, although other initial conditions produce similar behavior. In order to trace out the dependence of the recruitment level on the recruitment rate for the given rewiring rate w and to improve the rate of convergence to the steady state, we use the steady-state configuration of the system for the previous value of γ as the initial condition for the next value of γ. The time-averaged values are computed once the system reaches steady-state regimes, which is assumed to be reached after at least $10\,\delta^{-1}$ units of time, i.e., about ten generations of nodes have died before the system is assumed to be at the steady state. The measurements of $\mathcal{N}_R$ are performed by averaging over 100 dynamical states of the system.

In figures 2 and 3 we show the results of simulating the system in these two regimes. The density plots in figures 2(*b*) and 3(*b*) show the fraction of recruited nodes as a function of recruiting rate Γ and rewiring rate W in networks with $\Lambda_1 \gg 1$ and $\Lambda_1 \ll 1$ respectively. The black curves in the two figures represent the location of the recruiting threshold as derived from the mean-field equations and given by equation (8). Here mean field allows us to accurately predict the onset of the stable nontrivial solution. In figures 2(*a*) and 3(*a*) we compare the simulation results to the mean-field predictions. The recruiting threshold shows excellent agreement with the simulations. This is likely due to the fact that, as we approach

7

(a) (b)

Figure 3. Direct numerical simulation of a stochastic network system with $\Lambda_1 \ll 1$. In (a) we compare the result of the simulation to the mean-field solution given by equation (A.18). Square (red online): strong rewiring, $W \approx 70$. Circle (green online): weak rewiring, $W \approx 0.2$. (b) shows the density plot representing the dependence of the fraction of recruited nodes in the population in statistical steady state on rescaled rates of rewiring, W, and recruiting, Γ. Vertical solid line (green online) corresponds to the minimum recruitment rate required to support nontrivial solution, as given by equation (9). Horizontal dashed line (red online) corresponds to the rewiring rate that guarantees existence of a nontrivial solution in the limit of large recruitment rate (equation 10). The solid curve corresponds to the recruiting threshold as predicted by mean field in equation (8). The simulations are performed on a system with $\lambda_1 = 0.01$, $\lambda_2 = 10$, $\mu = 10^5$, $\delta = 1$, $\sigma = 10$.

the threshold, the expected number RS-links per S-node approaches zero, and the closures of equation (3) can be viewed as linear expansions of the triples in terms of $\mathcal{N}_{RS}/\mathcal{N}_S$. We also observe excellent agreement in the limit of large Γ, while the minor discrepancy near the bifurcation point is to be addressed in future publications.

We observe in simulations that the steady-state trivial solution undergoes a forward transcritical bifurcation in the recruiting rate Γ for all values of W for which a nontrivial solution exists. This is in contrast with epidemiological models where the purpose of the rewiring is avoidance of the nodes spreading infection [25, 24], which can undergo a backward transcritical bifurcation and exhibit bistability. Note that, unlike those models, the purpose of the rewiring in the recruitment model is attraction of the susceptible population by the recruiters.

We would like to draw the reader's attention to an important difference in the system behavior in the two regimes. In the regime where $\Lambda_1 \gg 1$, the nontrivial solution exists for all values of W as long as Γ is large enough. On the other hand, in the regime where $\Lambda_1 \ll 1$, the nontrivial solution may fail to exist for any value of Γ unless rewiring is aggressive enough. In figure 3(b) there is a range of rewiring rates W for which only trivial solutions exist. The horizontal dashed line, given by equation (10), indicates the mean-field level of rewiring that is *sufficient* for the nontrivial solution to exist for rapid recruiting (large Γ). Also, we can see that the rewiring level that is *necessary* for the emergence of the nontrivial solution can be very close to the predicted sufficient level of equation (10), for small values of Λ_1.

Another important difference between the two regimes of Λ_1 values is seen when we compare two systems with different values of Λ_1 and Λ_2 while the ratio $\Lambda_1/(1 + \Lambda_2)$ is kept fixed. Note that in the absence of recruitment, such systems have identical fractions of susceptible nodes. In other words, in the presence of recruitment, the pool of individuals available for recruitment would appear to be the same. However, as we can see from figure 4, there is a significant difference in the size of the recruited population as well as the recruiting threshold. The size difference at large recruiting rates appears to be caused by the difference
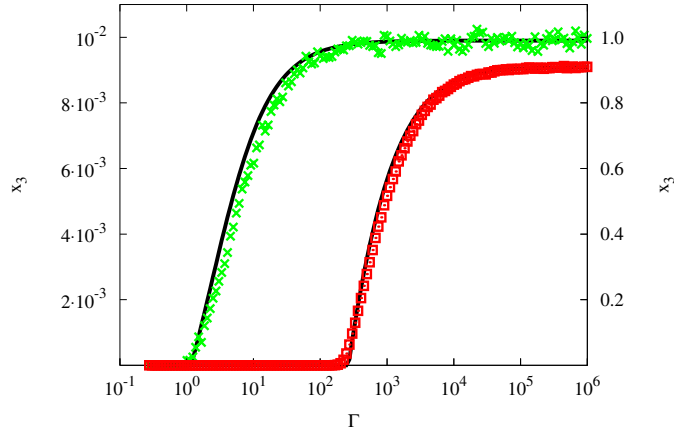
Figure 4. Comparing systems with different values of Λ_1, but same ratio of $\Lambda_1/(1+\Lambda_2)$. Squares (red online), right axis: $\Lambda_1 = 10$, $\Lambda_2 = 10^4$. Crosses (green online), left axis: $\Lambda_1 = 0.01$, $\Lambda_2 = 9.001$. Both of the simulations were performed with the following parameters: $w = 10$, $\mu = 10^5$, $\delta = 1$, $\sigma = 10$.

in the dynamics in the two regimes. Thus, for large values of Λ_1 and Λ_2 any node can become susceptible to recruitment several times during its life, while as the value of Λ_1 decreases, only some nodes will ever become susceptible, with low likelihood of doing so more than once. We also note that the small Λ_1, Λ_2 case has a lower threshold. This occurs because when a node becomes susceptible it remains that way for some time due to a small Λ_2, allowing some R-node to rewire to and recruit it. On the other hand, in the case of a very large Λ_2 the recruitment must be more aggressive in order to capture the S-node before it returns to the N-state.

3.3. Recruited subnetwork geometry

We now investigate the structure of the portion of the network (later referred to as the R-subnetwork) consisting only of R-nodes and links between them. In particular, we are interested in the mean degree of its nodes when the system reaches a steady state. The mean-field approach, in addition to predicting the fraction of recruited nodes (which corresponds to the size of the R-subnetwork), also provides information about topology of the subnetwork in the form of mean degree of the nodes. The mean degree of a node in the subnetwork serves as a low order description of how well the nodes in the network are connected, which may be important for communication within the established subnetwork. The density plot in figure 5 shows the dependence of the mean degree on W and Γ. The nonmonotonic behavior as a function of Γ for fixed W is predicted by the mean-field model. The solid line corresponds to the analytical prediction of the maximum's location as given by equation (B.4) derived in appendix B. Note that the analytic description of the maximum's location would allow the recruiting class to optimize connectivity within the subnetwork, if that happens to be an important goal for that class. The mean-field approximation fails to capture the nonmonotonic behavior of the mean degree in the limit where $\Lambda_1 \ll 1$, and we leave this issue to a future study.

In addition to the information that can be extracted directly from the mean-field equations, we complete the picture by presenting the numerical measurement of the degree distribution
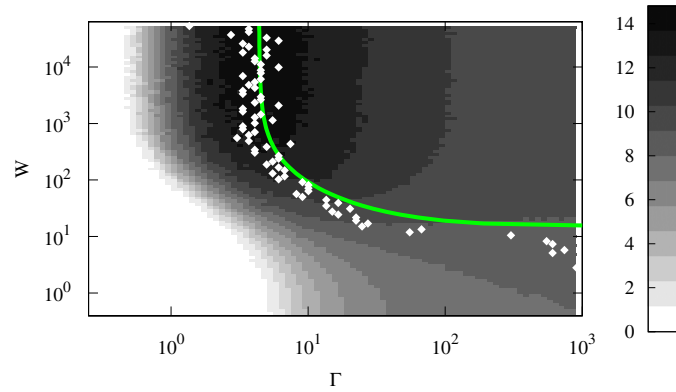
Figure 5. Direct numerical simulation. Density plot representing the dependence of the fraction of the mean node degree in the R-subnetwork in steady state, $2\mathcal{N}_{\mathrm{RR}}/\mathcal{N}_{\mathrm{R}}$, on rescaled rates of rewiring, W, and recruiting, Γ. Solid line (green online) indicates the value of Γ where the degree is at a maximum for a given value of W, found using analytic expression in equation (B.4). The white diamonds correspond to the location of the maximum in simulations for a given value of W. The simulations are performed with the following parameters: $\mu = 10^5$, $\delta = 1$, $\sigma = 10$, $\lambda_1 = 10$, $\lambda_2 = 100$.
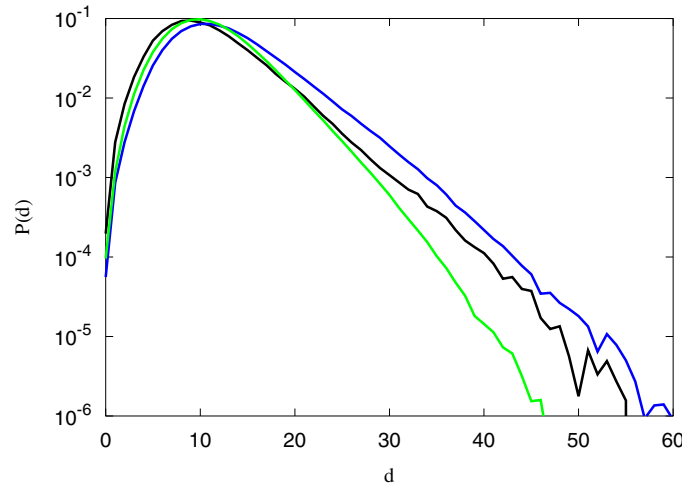
Figure 6. Degree distribution of nodes in the subnetwork of R-nodes (i.e., probability $P(d)$ for an R-node to have d R-node neighbors). Black (black online): $\Gamma = 10^{0.5}$, gray (blue online): $\Gamma = 10^1$, light gray (green online): $\Gamma = 10^2$. The simulations are performed with the following parameters: $\mu = 10^5$, $\delta = 1$, $\sigma = 10$, $\lambda_1 = 10$, $\lambda_2 = 100$, $w = 100$.

in the subnetwork formed of R-nodes. For this distribution the degree is defined as the number of R-nodes in the neighborhood of a given R-node. In figure 6 we can see that the degree distribution has an exponentially decaying tail.

4. Conclusions and discussion

We develop a toy model that describes recruitment of new members by an interested class within a society. The members of the recruiting class can increase the number of recruits via adaptation. Thus, they may choose to abandon their relations with those members of society

that are not prone to recruitment. This model assumes that once a node joins the recruiting class, it itself becomes a recruiter and it remains a member of this class until death. In contrast to avoidance rewiring used to reduce infection spreading in epidemic models [24, 25], network adaptation in our model promotes spreading. Additionally, the population is open with birth and death modeled explicitly, while most previous adaptive network models have been of closed populations (e.g., [24, 25, 28, 20–23]).

In this paper, we develop and analyze a mean-field description of our model. Thus, we are able to accurately predict the onset of the stable nontrivial solution of the system at steady state. Furthermore, we are able to accurately predict the size of the recruited class for a given set of system parameters, as well as the mean degree of the subnetwork formed by the recruited members. We compare the predictions made by the mean-field description with the direct simulations of our model. We generally observe a good agreement between the model and its mean-field approximation.

Analyzing the mean-field model, we find two parameter regimes with very distinct qualitative behavior. Thus, we show that in the society where the particular ideology is unpopular (perhaps corresponding to radical ideology) and individuals rarely become susceptible to it, adaptation is necessary in order to observe stable nonzero levels of the recruiting class. On the other hand, if the idea is sufficiently popular (e.g., recruitment into a moderate political party), the adaptation improves the recruiting capabilities and may affect the ultimate topology of the recruited, but adaptation is not a necessary condition for the existence of a nonzero stable solution. Furthermore, we speculate that if the model were changed to describe a society with two competing recruiting classes (think two-party system), the adaptation may be a mechanism by which one competing class gets an edge over the other class.

The ad hoc homogeneity assumption for closure of triples works fairly well because the mechanisms of the model do not introduce much correlation between a node and its neighbor's neighbor. However, as evidenced by the results presented in figures 2(*a*) and 3(*a*), the mean-field approximation has some inaccuracies in the parameter regime between the bifurcation point and the asymptotic saturation. This can also be seen via direct measurement of the number of triples of each type in simulations (data not shown). For example, the longer an S-node has been susceptible, the more R-nodes will have wired to it. Thus, high degree S-nodes will have disproportionately more R neighbors than will low degree S-nodes, affecting the number of RSR triples. In another work [29], we develop and analyze a new closure of the mean-field equations that more accurately describes the full system in various asymptotic regimes, such as fast rewiring.

Acknowledgments

Appendix A. Exact solution

In this appendix, we derive the exact solution to the system of equations in equations (1) and (2) when the system is at the nontrivial steady state, i.e., when the left-hand side of the equations

is zero and the size of recruiting class is nonzero. We begin by deriving the dimensionless equations, as defined in section 3.1:

$$\partial_{\tilde{t}} x_1 = 1 - \Lambda_1 x_1 + \Lambda_2 x_2 - x_1 \tag{A.1a}$$

$$\partial_{\tilde{t}} x_2 = \Lambda_1 x_1 - \Lambda_2 x_2 - \Gamma x_8 - x_2 \tag{A.1b}$$

$$\partial_{\tilde{t}} x_3 = \Gamma x_8 - x_3 \tag{A.1c}$$

$$\partial_{\tilde{t}} x_4 = \Lambda_2 x_5 + 2\frac{x_1}{x_1 + x_2 + x_3} - 2(\Lambda_1 + 1)x_4 \tag{A.1d}$$

$$\partial_{\tilde{t}} x_5 = 2\frac{x_2}{x_1 + x_2 + x_3} - \Gamma\frac{x_5 x_8}{x_2} + 2\Lambda_2 x_6 - (\Lambda_1 + \Lambda_2 + 2)x_5 + 2\Lambda_1 x_4 \tag{A.1e}$$

$$\partial_{\tilde{t}} x_6 = -2\Gamma\frac{x_8 x_6}{x_2} + \Lambda_1 x_5 - 2(\Lambda_2 + 1)x_6 \tag{A.1f}$$

$$\partial_{\tilde{t}} x_7 = \Gamma\frac{x_5 x_8}{x_2} + 2\frac{x_3}{x_1 + x_2 + x_3} - (\Lambda_1 + 2 + W)x_7 + \Lambda_2 x_8 \tag{A.1g}$$

$$\partial_{\tilde{t}} x_8 = -\Gamma\left(\frac{x_8^2}{x_2} + 2\sigma^{-1}x_8\right) + 2\Gamma\frac{x_6 x_8}{x_2} - (\Lambda_2 + 2)x_8 + (\Lambda_1 + W)x_7 \tag{A.1h}$$

$$\partial_{\tilde{t}} x_9 = \Gamma\left(\frac{x_8^2}{x_2} + 2\sigma^{-1}x_8\right) - 2x_9. \tag{A.1i}$$

At steady state, the left-hand side of the above equations is zero. We proceed in our derivation by dividing all equations in the steady state by x_2 and introducing a new variable $z_i \equiv x_i/x_2$, obtaining the following system of equations:

$$0 = 1/x_2 - \Lambda_1 z_1 + \Lambda_2 - z_1 \tag{A.2a}$$

$$0 = \Lambda_1 z_1 - \Lambda_2 - \Gamma z_8 - 1 \tag{A.2b}$$

$$0 = \Gamma z_8 - z_3 \tag{A.2c}$$

$$0 = \Lambda_2 z_5 + 2z_1 - 2(\Lambda_1 + 1)z_4 \tag{A.2d}$$

$$0 = 2 - \Gamma z_5 z_8 + 2\Lambda_2 z_6 - (\Lambda_1 + \Lambda_2 + 2)z_5 + 2\Lambda_1 z_4 \tag{A.2e}$$

$$0 = -2\Gamma z_8 z_6 + \Lambda_1 z_5 - 2(\Lambda_2 + 1)z_6 \tag{A.2f}$$

$$0 = \Gamma z_5 z_8 + 2z_3 - (\Lambda_1 + 2 + W)z_7 + \Lambda_2 z_8 \tag{A.2g}$$

$$0 = -\Gamma\left(z_8^2 + 2\sigma^{-1}z_8\right) + 2\Gamma z_6 z_8 - (\Lambda_2 + 2)z_8 + (\Lambda_1 + W)z_7 \tag{A.2h}$$

$$0 = \Gamma\left(z_8^2 + 2\sigma^{-1}z_8\right) - 2z_9. \tag{A.2i}$$

We have used the fact that in the steady state $x_1 + x_2 + x_3 = 1$, as can be shown by adding together equations (1a)–(1c). In the rest of the derivation we will find a closed equation for z_8 and express the other z_is in terms of z_8.

We can immediately express z_1, z_3, and z_9 in terms of z_8 by solving equations (A.2b), (A.2c) and (A.2i) respectively:

$$z_1 = \Lambda_1^{-1}(1 + \Lambda_2 + \Gamma z_8) \tag{A.3}$$

$$z_3 = \Gamma z_8 \tag{A.4}$$

$$z_9 = (\Gamma/2)\left(z_8^2 + 2\sigma^{-1}z_8\right). \tag{A.5}$$

We substitute equation (A.3) into equations (A.2d), and (A.4) into equation (A.2g). The resulting two equations, together with equations (A.2e), (A.2f) and (A.2h), form a closed system of five equations with five unknowns z_4–z_8.

We solve equation (A.2f) for z_5 in terms of z_6 and z_8:

$$z_5 = 2\Lambda_1^{-1}(1 + \Lambda_2 + \Gamma z_8)z_6, \tag{A.6}$$

and substitute the above result into equations (A.2d) and (A.2g), to solve for z_4 and z_7 in terms of z_6 and z_8 as follows:

$$z_4 = [(\Lambda_1 + 1)\Lambda_1]^{-1}[1 + \Lambda_2 + \Gamma z_8][1 + \Lambda_2 z_6] \tag{A.7}$$

$$z_7 = \left[\Gamma\Lambda_1^{-1}(2\Gamma z_8 + 2(\Lambda_2 + 1))z_6 + 2\Gamma + \Lambda_2\right](\Lambda_1 + 2 + W)^{-1}z_8. \tag{A.8}$$

Substituting the expressions for z_4 and z_5 from equations (A.6) and (A.7) into equation (A.2e), and solving for z_6 we obtain

$$z_6 = \frac{\Lambda_1}{\Gamma(\Lambda_1 + 1)z_8 + (\Lambda_1 + \Lambda_2 + 1)}. \tag{A.9}$$

Finally, substituting results of equations (A.9) and (A.8) into equation (A.2h) we obtain an equation for z_8 in a closed form:

$$\frac{[(a_1\Gamma)z_8^2 + (a_2\Gamma + a_3)z_8 + (a_4\Gamma^{-1} + a_5)]z_8}{[\Gamma(\Lambda_1 + 1)z_8 + (\Lambda_1 + \Lambda_2 + 1)]} = 0 \tag{A.10}$$

where

$$a_1 \equiv (\Lambda_1 + 1)(\Lambda_1 + W + 2) \tag{A.11}$$

$$a_2 \equiv 2\sigma^{-1}(\Lambda_1 + 1)(\Lambda_1 + W + 2) - 2(\Lambda_1 + 2)(W + \Lambda_1) \tag{A.12}$$

$$a_3 \equiv 3(\Lambda_1 + 1)(\Lambda_1 + W + 2 + \Lambda_2) + \Lambda_2(W + 1) \tag{A.13}$$

$$a_4 \equiv 2(\Lambda_1 + \Lambda_2 + 1)(\Lambda_1 + W + 2 + \Lambda_2) \tag{A.14}$$

$$a_5 \equiv (\Lambda_1 + \Lambda_2 + 1)[2(\sigma^{-1} - 2)(W + \Lambda_1) + 4(\sigma^{-1} - \Lambda_1)]. \tag{A.15}$$

Note that the physically relevant solutions are positive, and therefore finding a nontrivial solution of z_8 is a simple matter of solving a quadratic equation:

$$(a_1\Gamma)z_8^2 + (a_2\Gamma + a_3)z_8 + (a_4\Gamma^{-1} + a_5) = 0. \tag{A.16}$$

Solving equation (A.2a) for x_2, we can now express x_2 in terms of the newly found z_8:

$$x_2 = \Lambda_1[(\Lambda_1 + 1)\Gamma z_8 + (\Lambda_1 + \Lambda_2 + 1)]^{-1}. \tag{A.17}$$

The rest of the original variables can be found using $x_i = x_2 z_i$. Thus, for example, x_3 is

$$x_3 = x_2 z_3 = \Gamma\Lambda_1 z_8[(1 + \Lambda_1)\Gamma z_8 + (\Lambda_1 + \Lambda_2 + 1)]^{-1}. \tag{A.18}$$

Appendix B. Extremum of the mean degree in R-subnetwork

In steady state, the mean degree of the nodes within the R-subnetwork is found by taking a ratio of twice the number of RR-links to the number of R-nodes in the subnetwork:

$$\langle k \rangle = \frac{2\mathcal{N}_{RR}}{\mathcal{N}_R} = \frac{\mathcal{N}_{RS}}{\mathcal{N}_S} + 1 = \frac{\sigma}{2}z_8 + 1 \tag{B.1}$$

where the values of $\mathcal{N}_{RR}$ and $\mathcal{N}_R$ are obtained by solving equations (1*c*) and (2*f*) in steady state. In this appendix we determine the value of Γ, Γ_m, that for a given rewiring rate will maximize the degree in the resulting R-subnetwork. We do this by maximizing z_8.

Differentiating equation (A.16) with respect to Γ and evaluating the resulting equation at Γ_m, the value where extremum is attained, we obtain

$$a_1(z_8)_m^2 + a_2(z_8)_m - \Gamma_m^{-2}a_4 = 0. \tag{B.2}$$

Note that the derivative of z_8 with respect to Γ evaluated at Γ_m is equal to zero because z_8 is an extremum there, and the a_i are independent of Γ. Multiplying the above equation by Γ and subtracting it from equation (A.16) evaluated at Γ_m allows us to solve for $(z_8)_m$:

$$(z_8)_m = -\frac{2a_4 + \Gamma a_5}{\Gamma a_3}, \tag{B.3}$$

Substituting the value of $(z_8)_m$ into equation (B.2) and solving for Γ_m we obtain

$$\Gamma_m = \left[a_2 a_3 a_4 - 2a_1 a_4 a_5 + \left(a_2^2 a_3^2 a_4^2 + a_1 a_5^2 a_4 a_3^2 - a_2 a_3^3 a_5 a_4\right)^{1/2}\right] \Big/ [a_5(a_1 a_5 - a_3 a_2)], \tag{B.4}$$

the location of the maximum for the given rewiring rate.

References

[1] Meyer F and Ultsch A 2010 Finding music fads by clustering online radio data with emergent self-organizing maps *Advances in Data Analysis, Data Handling and Business Intelligence* (*Studies in Classification, Data Analysis, and Knowledge Organization*) (Berlin: Springer) pp 419–27
[2] Bendor J, Huberman B A and Wu F 2009 *J. Econ. Behav. Organ.* **72** 290
[3] Janssen M A and Jager W 2001 *J. Econ. Psychol.* **22** 745
[4] Abrahamson E 2009 *Scand. J. Manag.* **25** 235
[5] Grueter C and Ratnieks F 2011 *Anim. Behav.* **81** 949
[6] Benedict B 2007 *SIAM News* **40** (3) April 2007
[7] Kuhlman C J, Kumar V S A, Marathe M V, Ravi S S and Rosenkrantz D J 2010 Finding critical nodes for inhibiting diffusion of complex contagions in social networks *Machine Learning and Knowledge Discovery in Databases* (*Lecture Notes in Computer Science* vol 6322) (Berlin: Springer) pp 111–27
[8] Gutfraind A 2009 Terrorism as a mathematical problem *SIAM News* **42** (8) October 2009
[9] Gutfraind A 2009 *Stud. Confl. Terrorism* **32** 45
[10] Johnson N F, Spagat M, Restrepo J A, Becerra O, Bohrquez J C, Suarez N, Restrepo E M and Zarama R 2006 arXiv:physics/0605035
[11] Cherif A, Yoshioka H, Ni W and Bose P 2009 arXiv:0910.5272
[12] Johnson N, Carran S, Botner J, Fontaine K, Laxague N, Nuetzel P, Turnley J and Tivnan B 2011 *Science* **333** 81
[13] Caulkins J P, Grass D, Feichtinger D and Tragler G 2008 *Comput. Oper. Res.* **35** 1874
[14] Udwadia F, Leitmann G and Lambertini L 2006 *Discrete Dyn. Nature Soc.* **2006** 85653
[15] Bentson K 2006 *Master's Thesis* Air Force Institute of Technology
[16] Butler L B 2011 *SAMS Monograph: Technical Report* OMB No 074-0188 (Fort Leavenworth, KS: School of Advanced Military Studies)
[17] Lindelauf R, Borm P and Hamers H 2009 *Soc. Netw.* **31** 126
[18] Farley J D 2003 *Stud. Confl. Terrorism* **26** 399
[19] Bar-Isaac H and Baccara M 2006 How to organize crime *Working Papers 06-07* (New York: Department of Economics, Leonard N Stern School of Business, New York University)
[20] Benczik I J, Benczik S Z, Schmittmann B and Zia R K P 2008 *Europhys. Lett.* **82** 48006
[21] Benczik I, Benczik S, Schmittmann B and Zia R 2009 *Phys. Rev.* E **79** 046104

[22] Schmittmann B and Mukhopadhyay A 2010 *Phys. Rev.* E **82** 066104
[23] Holme P and Newman M E J 2006 *Phys. Rev.* E **74** 056108
[24] Gross T, D'Lima C J D and Blasius B 2006 *Phys. Rev. Lett.* **96** 208701
[25] Shaw L B and Schwartz I B 2008 *Phys. Rev.* E **77** 066101
[26] Gillespie D 1976 *J. Comput. Phys.* **22** 403
[27] Keeling M J, Rand D A and Morris A J 1997 *Proc. Biol. Sci.* **264** 1149
[28] Gross T and Blasius B 2008 *J. R. Soc. Interface* **5** 259
[29] Shkarayev M S and Shaw L B 2013 arXiv:1304.1816